Cellulose (2021) 28:4701–4718
https://doi.org/10.1007/s10570-021-03835-5

ORIGINAL RESEARCH

Biocompatibility and selective antibacterial activity of a bismuth phosphinato-nanocellulose hydrogel

Maisha Maliha · Rajini Brammananth · Jennifer Dyson · Ross L. Coppel · Melissa Werrett · Philip C. Andrews · Warren Batchelor

Received: 9 November 2020 / Accepted: 16 March 2021 / Published online: 29 March 2021

Abstract Antimicrobial hydrogels are of immense value in wound care applications. However, the rapid rise of antimicrobial resistance has made it necessary to look for new antimicrobial additives for such materials. In this study, a novel antimicrobial hydrogel for wound care applications has been developed. The material combines TEMPO-oxidized nanocellulose hydrogel with a new class of antimicrobial agent, phenyl *bis*-phosphinato bismuth (III) complex. The hydrogel was characterized using scanning electron microscope imaging to show the overall distribution of the complex particles within the nanocellulose hydrogel matrix phase. The rheological properties of the bismuth loaded hydrogel are comparable to commercial over-the-counter burn hydrogels and behave like true gels. Activity of the different concentrations of the complex was studied against a range of medically important bacteria and mammalian fibroblast cells. Bismuth complex target loading of 9 µg/g showed bactericidal activity against *Acinetobacter baumannii* and *Pseudomonas aeruginosa* and bacteriostatic effect against MRSA and VRE, while having no toxic effect on mammalian fibroblast cells. However, *Escherichia coli* was less susceptible to this concentration comparatively. Our study has identified a range of bismuth complex loading levels for the material at which the additive appears to be safe and active. This study is a step towards the design of a biocompatible and renewable hydrogel containing a safe antimicrobial additive, which has an excellent safety margin to pathogenic bacteria over mammalian cells and would appear to be a promising material for active wound dressing applications.

Supplementary Information The online version contains supplementary material available at https://doi.org/10.1007/s10570-021-03835-5.

M. Maliha · W. Batchelor (✉)
Department of Chemical Engineering, Bioresource Processing Research Institute of Australia (BioPRIA), Monash University, Clayton, VIC 3800, Australia
e-mail: warren.batchelor@monash.edu

R. Brammananth · R. L. Coppel
Department of Microbiology, Monash University, Clayton, VIC 3800, Australia

J. Dyson
Monash Institute of Medical Engineering (MIME), Monash University, Clayton, VIC 3800, Australia

J. Dyson
Department of Biochemistry and Molecular Biology, Monash Biomedicine Discovery Institute, Monash University, Clayton, VIC 3800, Australia

M. Werrett · P. C. Andrews
School of Chemistry, Monash University, Clayton, VIC 3800, Australia

M. Werrett · P. C. Andrews
Centre To Impact AMR, Monash University, Clayton, VIC 3800, Australia

Graphic abstract

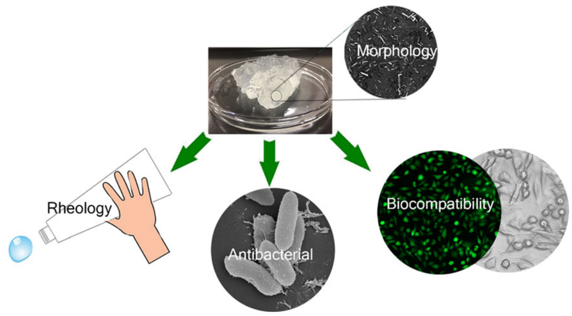

Keywords Nanocellulose · Bismuth · Hydrogel · Antibacterial · Fibroblasts · In-vitro cytotoxicity

Introduction

Skin is the largest organ of the human body, protecting all internal organs. Trauma to the skin breaches this protective layer and exposes internal structures to the risk of infection and other forms of damage. The repair of skin in which the integrity of this layer is restored involves three phases: inflammation, proliferation of various cell types, and tissue remodeling. The initial inflammatory phase involves the action of preformed proteins and resident and migratory cells to sterilise the area of the wound in preparation for a proliferative phase in which subcutaneous and dermal cells proliferate to generate new skin layers including new blood vessels. Finally, the newly generated tissues are remodeled to regenerate the various layers of the skin and to integrate with the pre-existing tissues on either side of the wound. Disruption in any one phase of repair can jeopardise the satisfactory completion of the process (Agyingi et al. 2010). A large number of factors including infection can affect wound healing and control of infection is a pre-requisite for satisfactory wound healing (Caló and Khutoryanskiy 2015; Jones et al. 2006). Bacterial infection in burn wounds complicates their management and in the worst cases can lead to the death of patient (Rattanaruengsrikul et al. 2009). Technologies to deal with wound management include artificial skin for grafting, aids to skin regeneration and wound closure, and infection control by various exogenous materials and dressings (Ashtikar and Wacker 2018). A large number of wound dressings have been developed, both from natural and synthetic materials (Hakkarainen et al. 2016). Active wound dressings that deliver drugs or contains antibacterial agents are commonly used to minimise risk of infection (Rattanaruengsrikul et al. 2009). Bacteria are constantly evolving and developing increased resistance to antibiotics and disinfectants and appropriate dressings need to be developed to account for this. In addition, wound dressing materials need to be biocompatible and non-toxic to host cells (Basu et al. 2018).

Hydrogel-based wound dressings are some of the most promising materials for wound care and healing due to their "tissue-like" structure and excellent biocompatibility (Kamoun 2017). The frequency of application of hydrogels in wound dressings has increased due to its ability to provide a moist environment to assist in the wound healing process (Rattanaruengsrikul et al. 2009). Moisture helps with dermis repair and removal of dead cells, thus aiding in healing. Moreover, the moisture provides a cooling effect on the wound, reducing pain. Pain is also reduced due to the non-adherent nature of hydrogels preventing sticking to the wound when dressings are removed (Basu et al. 2017). Hydrogels have the ability to absorb the wound exudates and are also permeable to oxygen, making the properties of hydrogels further advantageous for wound dressing (Singh and Singh 2012).

Hydrogels are three-dimensional structures of crosslinked polymers. For biomedical applications, physically cross-linked hydrogels are preferred as they avoid the use of chemical crosslinking agents or organic solvents, thus minimizing the risks and toxicity associated with those (Kamoun 2017). One such material is nanocellulose hydrogel, which is crosslinked by hydrogen bonding and is a promising material for biomedical applications (De France et al. 2017). The surface chemistry of nanocellulose has been studied and reported to be suitable for wound dressing applications (Chinga-Carrasco and Syverud 2014). Cellulose-based hydrogels studied for wound dressing applications are usually bacterial cellulose. Nanocellulose-based wound care products, such as Biofill, Gengiflex and XCell, are also based on bacterial cellulose (BC) (Czaja et al. 2006; Laçin 2014). Bacterial cellulose (BC) and wood-based cellulose has the same chemical structure with the same sugar molecule forming the polymer. However, BC is a weak hydrogel and is hard to modify to other forms (Hakkarainen et al. 2016), and the large scale production of bacterial cellulose remains a challenge (Czaja et al. 2006). There has been limited research exploring the application of wood-based nanocellulose in wound dressings. Hakkarainen, Koivuniemi et al. studied the use of wood-based nanocellulose as wound dressing for burns in patients (Hakkarainen et al. 2016), leading to the first wood-based nanocellulose hydrogel, recently launched to the European market as a wound care product by UPM-Kymmene Corporation (Finland: UPM's FibDex, a wood-based innovation for wound care, receives regulatory approval and CE mark 2019). Of relevance to this study, the effect of antimicrobials combined with wood-based nanocellulose hydrogels is yet to be investigated.

In this study, wood-based nanocellulose hydrogel incorporating a metal-based antimicrobial agent has been studied. Silver nanoparticles and silver-based compounds are common antimicrobial additives used for wound dressing applications. These have been studied as antimicrobial agents in hydrogels assembled with both synthetic polymers (Abou-Yousef and Kamel 2015; Bardajee et al. 2012; González-Sánchez et al. 2015; Resmi et al. 2017; Singh and Singh 2012; Thomas et al. 2007; Tyliszczak et al. 2017; Valle et al. 2014) and natural polymers (Babu et al. 2010; Hebeish et al. 2013; Rattanaruengsrikul et al. 2009). Bacterial cellulose hydrogel has also been impregnated with silver nanoparticles and the material displays antibacterial activity against both Gram-positive and Gram-negative bacteria (Maneerung et al. 2008). However, due to the overuse of silver in a large number of products, bacterial resistance towards silver has become a major concern (Gunawan et al. 2017; Maillard and Hartemann 2013; Silver 2003). It has also been reported that silver compounds, such as silver nitrate and the most commonly used silver sulfadiazine, can have a toxic effect in the human body (Restuccia et al. 2016 ; Maillard and Hartemann 2013; Rattanaruengsrikul et al. 2009; Stensberg et al. 2011). Furthermore, there are concerns about a build-up of silver in the environment and a desire to restrict its widespread use because of toxicity to various organisms, including humans (Werrett et al. 2018).

Researchers have shown that bismuth compounds and complexes possess antibacterial activity (Domenico et al. 2001; Kotani et al. 2005; Luqman et al. 2016; Svoboda et al. 2010; Werrett et al. 2018). In addition, bismuth compounds, such as bismuth *sub*salicylate (Pepto-Bismol) and colloidal bismuth subcitrate (De-Nol) have been used for treating gastrointestinal disorders (Barry and Sadler 2013; Briand and Burford 1999; Suzuki and Matano 2001). Moreover, bismuth and its compounds, unlike other heavy metals, are low in toxicity (Kotani et al. 2005) (Suzuki and Matano 2001). In this study, a Bi (III) complex with phosphinate ligands, $BiPh(OP(=O)Ph_2)_2$ is studied as an additive to a wound dressing hydrogel. While the antibacterial activity of this hydrophobic complex (Werrett et al. 2018) as well as the production of bismuth-nanocellulose composite sheets as an antimicrobial packaging material (Maliha et al. 2019) has been previously studied, the suitability of its incorporation into a hydrogel matrix for wound healing purposes is not known.

The aim of this study is to combine the new organobismuth complex, phenyl bismuth *bis*(diphenylphosphinato), into a nanocellulose hydrogel matrix to impart antibacterial properties to the hydrogel. The antibacterial properties of the hydrogel towards some of the medically important bacteria that commonly infect wounds has been studied. The rheological properties of the hydrogel were investigated and compared to commonly used commercial burn hydrogels. Moreover, biocompatibility of the hydrogel with mammalian fibroblast cells was studied to understand the overall safety of the composite.

Materials and methods

Chemicals and materials

Bleached Eucalyptus Kraft (BEK) pulp was obtained from Australian paper, Maryvale. 2,2,6,6-Tetramethylpiperidine-1-oxyl (TEMPO) and NaBr were obtained from Sigma-Aldrich. 12 w/v% Sodium hypochlorite (NaOCl) was purchased from Thermo Fisher Scientific. Triphenyl bismuth ($BiPh_3$) was prepared using the standard Grignard method (Barton et al. 1986) and diphenyl phosphinic acid was purchased from Sigma-Aldrich. NaOH and HCl were purchased from Merck and Univar, and diluted as required. Dulbecco's modified Eagle medium (DMEM) was purchased from Gibco. MTS reagent was purchased from Promega, Australia. Calcein, AM and Propidium iodide was obtained from Life technologies, Australia.

Preparation method

Bismuth complex synthesis

Phenyl bismuth *bis*(diphenylphosphinato) was prepared according to Andrews et al. (Werrett et al. 2018). Triphenyl bismuth and diphenyl phosphinic acid were mixed in the ratio of 1:2 in ethanol and heated at reflux for 24 h. The reaction mixture was then filtered, and the insoluble phenyl bismuth *bis*(diphenylphosphinato) was isolated as a white powder.

Preparation of bi-nanocellulose hydrogel

BEK pulp was oxidised by TEMPO-mediated oxidation as described by Isogai et al. (Saito et al. 2007). TEMPO (0.4 g) and NaBr (2.5 g) were mixed with water to which a suspension containing 25 dry grams of BEK pulp was added. This 3 L reaction mixture was initiated using 75 mL NaOCl added dropwise while being continuously stirred using an overhead stirrer. The NaOCl was pre-adjusted to pH 10 using 36% HCl. The reaction mixture was also maintained at pH 10 through the dropwise addition of 0.5 M NaOH. The oxidation was carried out for 2 h. The oxidised fibres were then dewatered and washed several times using vacuum filtration. The TEMPO-oxidised cellulose nanofibres thus obtained were then dispersed in deionised water to a concentration of 2 wt% and passed through the high-pressure homogeniser (GEA Niro Soavi Homogeniser Panda) at 1000 bar with one pass. Fibres produced similarly have been reported to have diameters in the range of 3–4 nm (Fukuzumi et al. 2009).

The desired mass of bismuth complex was dispersed in DI water using a dispermat at a speed of 6000 rpm for 15–25 min to ensure uniform dispersing of the complex. The dispersion was mixed with the 2 wt% nanocellulose (NC) hydrogels in 1:1 ratio and dispersed using the dispermat at 4000 rpm for 5 min. The Bi-NC hydrogel thus obtained had 0.1 wt% bismuth complex with respect to mass of hydrogel and was stored at 4 °C for further analysis. Blank hydrogel was prepared by mixing 2 wt% hydrogel with DI water in 1:1 ratio.

Morphology

The bismuth distribution in the hydrogel was analysed using Scanning Electron Microscope (SEM) imaging. The hydrogel was air-dried on a silicon chip secured using carbon tape. The hydrogel film was coated with a thin conducting layer of iridium. SEM imaging was done using the FEI Magellan 400 FEG SEM using an accelerating voltage of 5 keV and spot size 2.

Rheology

Rheological tests were done using Anton Paar MCR302 rheometer with the 1-degree cone and plate geometry. The analysis was done at 25 °C. Oscillatory strain sweep was performed at a constant frequency of 1 Hz at shear strains ranging from 0.01 to 100%.

In-vitro biocompatibility

Cytotoxicity assay

The cytotoxicity assay was performed according to modified ISO 10993-5. Mouse fibroblast L929 cells were cultured in Dulbecco's Modified Eagle's Medium (DMEM) containing 10% (v/v) fetal bovine serum (FBS) and 1% antibiotics (penicillin, streptomycin) in a humidified incubator at 37 °C and 5% CO_2. 10,000 cells/well were seeded into 96 well plates in DMEM medium and incubated for 24 ± 1 h to form a monolayer. The media was removed and cells washed with PBS. Fresh media mixed with the hydrogel samples was incubated with the cells. The 0.1 wt% hydrogel (containing 1000 µg Bi-complex/g hydrogel) was first dispersed in DMEM to contain 20 wt% hydrogel using a vortex mixture. This mixture was pipetted to further ensure homogenous distribution and then serially diluted with DMEM to test concentrations of 100, 50, 25, 12, 9, 6, 3, and 1 µg/g of the bismuth complex (rounded to the nearest whole number). The control cells were incubated with either fresh DMEM (negative control) or fresh DMEM containing 10% dimethyl sulfoxide (DMSO) to induce cell death (positive control). A similar set of experiments was undertaken using 0.1 wt% silver sulfadiazine loaded nanocellulose hydrogel in the same concentration range as the Bi-complex. DMEM containing 20 wt% blank nanocellulose hydrogel or commercial hydrogels were also tested. These were the two non-active over-the counter hydrogels, Solosite® and Solugel®, and silver-based active hydrogel, Silvasorb® and are referred to as commercial hydrogel **1**, commercial hydrogel **2** and commercial hydrogel **3** respectively in the paper. Cell viability was assessed after 24 h of treatment by MTS assay. The treatment media was replaced by MTS stock solution, when tetrazolium compound MTS is converted to formazan by viable cells. After 1 h of incubation in the dark, the absorbance was recorded using a Thermo Scientific Multiskan Spectrum plate reader at 490 nm and using the software SkanIt RE 2.4.2. The absorbance was corrected by subtracting the background absorbance, i.e. DMEM only in TCPS (tissue culture polystyrene) and was normalised against the negative control, i.e. the untreated cells grown on TCPS with fresh DMEM media, to express the absorbance in percentage of viability relative to the negative control. Four independent sets of experiments were performed with triplicates of each samples every time.

Live-dead assay

The live-dead assay was performed in a 96 well plate seeded with 10,000 cells/well and allowed to form a monolayer for 24 ± 1 h in 37 °C and 5% CO_2 condition. Cells were treated with media mixed with the hydrogel samples (with the same concentrations achieved by serial dilution as described above in "Cytotoxicity assay" section) and incubated for 24 h. The staining solution was prepared by mixing 6 drops of propidium iodide (PI) and 2 μL of Calcein AM to 3 mL PBS. The treatment media was replaced by staining solution and incubated in the dark for 30 min. Live-dead imaging was performed using the fluorescent microscope Nikon Eclipse Ts2 at 560 nm and 470 nm for Calcein AM and PI respectively.

Cell Morphology

A monolayer of L929 cell line in a 96 well plate seeded with 10,000 cells/ well was treated with different concentrations of the bismuth complex in a similar way as above in "Cytotoxicity assay" section, and incubated at 37 °C and 5% CO_2 condition for 24 h. The morphology of the cells was observed using light microscopy using the microscope Nikon Eclipse Ts2.

Statistical analysis

The MTS assay results were statistically analysed by one-way analysis of variance (ANOVA), followed by Tukey's post hoc test to compare selected pairs of data using GraphPad Prism 8.0.2. Tests with p values < 0.05 were considered to be statistically significant.

Antibacterial activity

Time-kill assay

Different amounts of 0.1 wt% Bi-loaded hydrogel was mixed with 5 mL of diluted overnight culture (1 in 100,000) of a specific bacterium such as to achieve concentrations of 12 μg, 9 μg, 6 μg and 3 μg of bismuth complex per gram of the broth (assuming density of broth as 1 g/ml). The time-kill assay of these different concentrations was performed against *Acinetobacter baumannii* (C403/ATCC17978), *Pseudomonas aeruginosa* (ATCC27853), *Escherichia coli* (G102), MRSA (M118797, methicillin-resistant *Staphylococcus aureus*) and Vancomycin-resistant *enterococcus* (M846910). Luria–Bertani (LB) media and LB agar plates were used for growing each of the bacterial line. The culture was spread on agar plate at the beginning of the experiment for time zero count. A vortex shaker was used to ensure proper mixing of the hydrogel with the broth. The suspension was kept in an incubator at 37 °C at 200 rpm shaking for 24 h and samples were aliquoted out after 4, 8, 12 and 24 h. 20 μL of the sample was plated on agar plates and the number of viable cells was determined by the colony counting technique. Each time point was analysed in triplicate, and each experiment was done three times.

Bacterial cell morphology

The morphology of bacterial cells after being treated was studied using SEM. The Bi-loaded hydrogel was mixed with 5 mL of diluted overnight culture (1 in 100,000) of *P. aeruginosa*, as described above, to obtain concentrations of 12 μg and 9 μg of bismuth complex per gram of the broth. These, along with a control, were incubated for 24 h at 37 °C. The treated culture was then centrifuged at 2000 rpm for 30 min at

4 °C. The supernatant was discarded and the pelleted cells were used for SEM sample preparation. The cells were washed with PBS and fixed using 2.5% glutaraldehyde and 2% paraformaldehyde for 1 h at room temperature. The fixed cells were then washed with fresh sodium cacodylate buffer and post-fixed with 1% osmium tetroxide in cacodylate buffer. The cells were then washed with milli-Q water and incubated on coverslips coated with 0.1% polyethyleneimine for 45 min. The coverslips were immersed in water to get rid of the unadhered cells, and treated with increasing concentrations of ethanol for dehydration. The coverslip was then critically point dried, mounted on SEM stub and coated with a thin conducting layer of gold. The SEM imaging was performed using FEI Nova NanoSEM.

Internal quality control

Quality control tests were done to evaluate the reliability and reproducibility of the antibacterial test results. Blinded experimental repeats of the time-kill assays were performed against MRSA (M118797, methicillin-resistant *Staphylococcus aureus*) and *Acinetobacter baumannii* (C403/ATCC17978). One sample contained the Bi-loaded hydrogel to achieve a concentration of 9 μg/g and another one contained the same amount of blank hydrogel as the control. The samples were analysed at 4 and 24 h and each time point was analysed in triplicate. The experiment was performed in the same way as before, except the test and the blank (control) samples were blinded.

Hydrogel quality check

Bismuth content analysis were carried out using a PerkinElmer Avio 200 Inductively Coupled Plasma - Optical Emission Spectrometer (ICP-OES), measuring Bi at 223.06 nm. Known masses from different batches of Bi-loaded hydrogels were ashed in a muffle furnace, wherein the temperature was ramped to and maintained at 600 °C for 3 h. The ash was then digested in concentrated nitric acid and diluted using 3% nitric acid. The elemental bismuth content was analysed and used to determine the bismuth complex content. Each batch of hydrogel was tested in triplicate and the mean mass of the bismuth complex per gram of hydrogel was reported.

Results and discussion

Morphology

Figure 1a and b shows the SEM images of the same area of the Bi-loaded hydrogel films. The secondary electron image in Fig. 1a shows the surface morphology only. In the back-scattered electron image (BSE) in Fig. 1b, the bright structures indicate the presence of higher atomic number element, which is bismuth. The main point of interest in these images is the distribution of the bismuth complex.

The bismuth particles have been shown to be well distributed within the nanocellulose fibres. Few bundles of fibres were observed, which is more closely shown in Fig. 1c. Those bundles that were present could be due to only having a single pass in the homogeniser in preparation of the gel. Better fibrillation can be achieved by more extensive mechanical treatment, although this would only be worthwhile if it led to a more active gel or was needed to satisfy regulatory requirements. Despite the presence of the bundles, the BSE image in Fig. S1 in supplementary data shows that the bismuth complex particles are sitting in between the nanofibres in the fibre bundle.

Rheology

To understand how the physical properties of the hydrogel are altered upon incorporation of the bismuth complex, its rheological properties were assessed. The complex viscosity plot shown in Fig. 2 indicates that the viscosity profile of the Bi-loaded hydrogel is similar to that of the blank hydrogel, showing a clear yield point for both and thereby suggesting the shear thinning behaviour of the hydrogel is retained. The dynamic strain sweep in Fig. 3 shows the elastic modulus G' (solid-like properties) and the viscous modulus G" (liquid-like properties). For hydrogels, the elastic modulus should be higher than the viscous modulus (Mendoza et al. 2018), which is consistent with our results. A rise of the zero-shear complex viscosity and storage modulus was observed with Bi-complex loading, suggesting the presence of the bismuth complex does not negatively affect the inter-fibre network. Although it has previously been observed that bismuth particles interfere with fibre–fibre bonding and upset the mechanical properties of nanocellulose paper (Maliha et al. 2019), the opposite

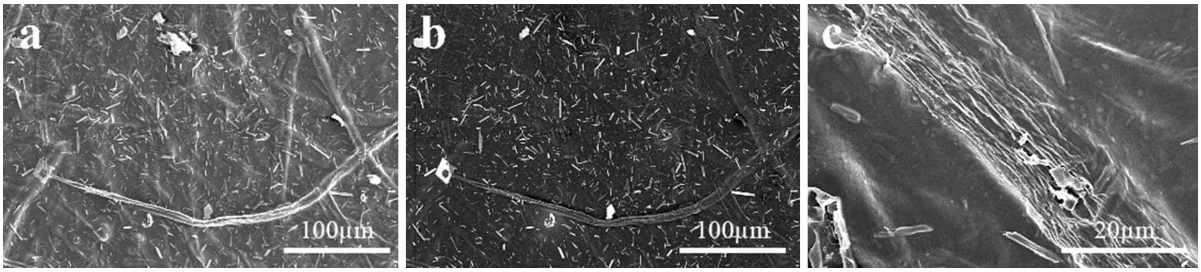

Fig. 1 SEM image of air-dried Bi-NC hydrogel. **a** Secondary electron image **b** Back-scattered electron image of the same area **c** secondary electron image showing a nanofibre bundle

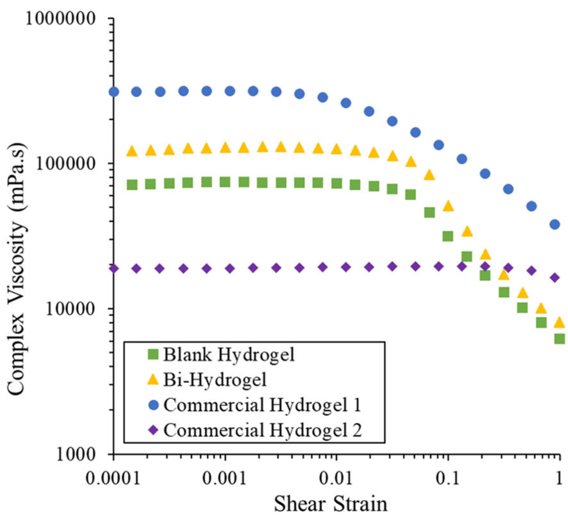

Fig. 2 Viscosity profile of blank hydrogel and bismuth-complex loaded hydrogel compared to commercial wound hydrogel

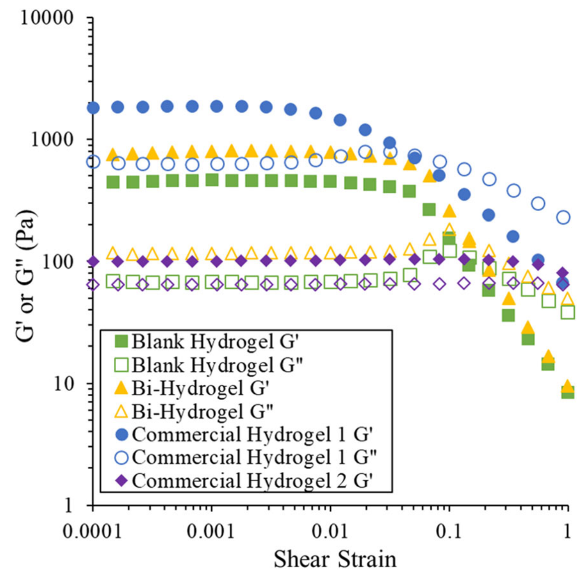

Fig. 3 Dynamic strain sweep of blank hydrogel and bismuth-complex loaded hydrogel compared to commercial wound hydrogel

is evident here. Figures 2 and 3 also show the complex viscosity and the modulus of two commercially available over-the-counter non-active wound hydrogels.

The rheological analysis show that the incorporation of bismuth does not affect the viscoelastic properties of the hydrogel and that the hydrogel behaves like a true gel. The blank nanocellulose hydrogel and the Bi-NC hydrogel showed G' higher than G'' at low shear strains and showed a linear viscoelastic region (LVR). These hydrogels have more solid-like properties at these strains and the G' and G'' remains independent of the change in strain. Beyond a certain strain, the viscous behaviour starts to take over. This is the critical strain beyond which the viscosity changes with shear and behaves like a non-Newtonian fluid. Thus, these can be used as free-flowing gels and have the capacity to be packaged in tubes as soft solids having an entangled fibrous network. The high zero shear viscosity tells us about the stability and the solid-like behaviour of the hydrogel during storage suggesting there is little possibility of sedimentation or phase separation. The higher elastic modulus and the zero-shear viscosity after the addition of the bismuth complex indicates stronger network formation. It can be speculated that the bismuth complex particles are taking part in the physical chain entanglement. Hence due to these particles being able to arrange themselves within the network, the material becomes less flexible and stiffer increasing the shear force required for the material to start flowing. The loss factor, tan δ, can be calculated as the ratio of the loss modulus to storage modulus and was found to be 0.15 for both the blank hydrogel and the Bi-hydrogel in the LVR. Moreover, the viscoelastic behaviour of the Bi-nanocellulose hydrogel studied here is comparable to commercial burn hydrogels as its elastic modulus and zero shear viscosity lies in the range of commercial brands investigated. Also, the critical strain for both the blank and Bi-complex loaded nanocellulose hydrogel is 0.068 and lies in between the range of the two commercial ones (0.003 and 0.347 for commercial hydrogel **1** and **2**, respectively). The yield point represents the ease of squeezing the gel out of a tube and the shear-thinning behaviour predicts the spreadability on shear forces for topical applications. These properties are important aspects for potential commercial translation. However, if required, the rheological properties of our Bi-hydrogel composites can be altered by changing the cellulose content of the hydrogel, as reported by Mendoza et al. (Mendoza et al. 2018).

In-vitro biocompatibility

Cytotoxicity assay

To determine whether the bismuth hydrogels are cytotoxic, several approaches were undertaken. Firstly, an MTS assay was employed to determine the viability of mouse fibroblast L929 cells that had been incubated with bismuth hydrogels, and the percentage cell viability determined relative to untreated cells i.e. cells grown in DMEM only. Statistical analysis was carried out using a 1-way ANOVA and a post-hoc Tukey's test. Fig. 4 shows a concentration-dependent effect of bismuth hydrogels on the viability of L929 cells. Generally, cell viability was unaffected by lower bismuth concentrations in the hydrogel, however, reduced cell viability was observed at higher concentrations. At bismuth complex concentrations greater than 12 μg/g, the mean normalised cell viability relative to the untreated control cells is below 20 %, indicating a cytotoxic effect of the complex as per the requirements of ISO 10993-5 standard. The standard identifies any medical device or material that leads to cell viability less than 70 % as cytotoxic. At concentrations $\leq$ 12 μg/g, the mean normalised cell viability was 70 % or greater, demonstrating a dose response curve for viability. Supporting this contention, at bismuth complex concentrations $\leq$ 12 μg/g, the mean normalised cell viability was not statistically different to that of untreated cells. This type of dose-dependent phenomenon was also seen with the silver sulfadiazine loaded hydrogel. Viability was significantly reduced when cells were cultured on high concentrations of silver in a dose-dependent manner. For example, concentrations $\leq$ 6 μg/g, silver sulfadiazine were not cytotoxic. We compared the toxicity of the blank nanocellulose hydrogel to commercial hydrogels in Fig. 4b. Commercial hydrogel 1 and 2 are non-antibacterial products. Commercial hydrogel 3 is a silver based antimicrobial hydrogel, that releases silver ions. The silver content of this hydrogel was studied using ICP-OES analysis and it was found to contain 3.81 $\pm$ 0.40 μg/g of equivalent silver sulfadiazine (1.15 $\pm$ 0.12 μg/g Ag^{+}). The silver content is well below the toxic limit observed herein. Surprisingly, all three of the commercial hydrogels showed a degree of cellular toxicity with viability counts far below 70 %. Nonetheless, these products are in clinical use and this suggests that in-vitro experiments may differ from a real-life scenario. There are a number of possible reasons for this. Monolayers of cells have only 15 % of cell contact as the cell density is lower than 1 % compared to normal skin tissue and extracellular content is very much different in the culture dish. Moreover, in-vitro experiments only deal with one cell type, in our case the fibroblast, and cell-cell interactions between different cell types in skin tissue is not taken into consideration (Hartung and Daston 2009). Skin tissue does not only consist of fibroblasts, but a number of different kinds of cells in various layers of skin including keratinocytes, Langerhans cells, melanocytes and vascular networks of blood vessels, sebaceous glands, nerves and many proteins like collagen (Shpichka et al. 2019). These along with the difficulty in understanding the reaction of the tissue to a foreign material or stress situation results in the difference in behaviour of cells in isolated cultures compared to when in the organism. Thus, it is difficult to extrapolate the in-vitro effects to in-vivo performance (Ghallab 2013). Moreover, the commercial hydrogels contain a range of other components (preservatives like parabens, imidazolidinyl urea etc.), some of which could also be the cause of the in-vitro cytotoxicity (Güzel Bayülken and Ayaz Tüylü 2019; Spindola et al. 2018).

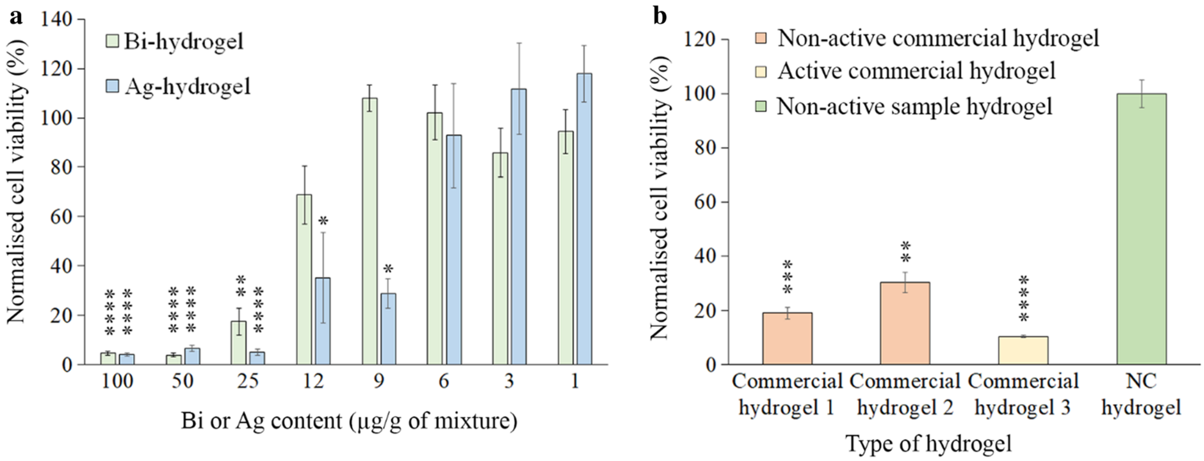

Fig. 4 Viability of L929 cells after treatment with **a** nanocellulose hydrogels loaded with the indicated target concentrations of Bi-complex (green) or Ag-compound (blue) and **b** the indicated commercial hydrogel and blank nanocellulose hydrogel, determined by MTS assay. Percentage viability normalised over no treatment DMEM control. The data presented are expressed as mean ± standard error of mean of technical triplicates from four independent sets of biological replicates. The number of asterisks over the bars show the level of significance of the data when compared with no treatment control. *$p \leq 0.05$, **$p \leq 0.01$, ***$p \leq 0.001$ and ****$p \leq 0.0001$

Live-dead assay

As an alternative approach for evaluating the potential cytotoxicity of bismuth-loaded hydrogels, a live-dead assay was undertaken. This assay employs two fluorescent probes—propidium iodide (PI) and calcein AM. PI is a red fluorescent nucleic acid stain that is only able to pass through the compromised membranes of non-viable cells, resulting in red nuclear fluorescence in dying or dead cells. Calcein AM is a cell membrane permeant fluorogenic substrate that is hydrolysed by active esterase in viable cells, resulting in a green cytosolic fluorescence in live cells. Figure 5 shows the L929 cells incubated with hydrogels loaded with various bismuth complex concentrations and stained with PI and calcein AM. Notably, at bismuth concentrations ≥ 12 ug/g the majority of cells were positive for PI indicating a cytotoxic affect, however, ≤ 9 ug/g most of the cells were positive for calcein and negative for PI suggesting lower bismuth concentrations do not significantly compromise cellular viability of this particular cell line. In control studies, the L929 cells were incubated with either the blank nanocellulose hydrogel (NC-gel) lacking bismuth, or DMEM cell culture media, and both conditions were associated with high levels of cell viability.

Cell morphology

Cell health and viability is intimately linked to cell morphology. Indeed, the induction of cell death is associated with distinct morphological events including cell shrinkage, plasma membrane blebbing and fragmentation. We examined the effect of increasing concentrations of the bismuth complex on the morphology of L929 cells (Fig. 6). Notably, a significant change in cell morphology indicating the induction of cell death was apparent at bismuth treatment concentrations above 9 μg/g, which is consistent with our observations in the cytotoxicity assays. At higher bismuth complex concentrations, the cells appeared smaller and more circular compared to the control cells cultured with a blank hydrogel (NG-gel) or in DMEM media. In addition, some cells displayed blebbing of the peripheral membrane (Fig. 6 see inset at 25 μg/g Bi-complex treatment). Following treatment with lower concentrations of the bismuth complex (9 μg/g), the cell size appeared unaffected, and the cell morphology was spindle shaped, similar to the control cells (NC-gel and DMEM). Thus, at or below bismuth complex concentrations of 9 μg/g, the presence of the complex in the hydrogel does not appear to affect the cell morphology.

The process of wound healing is highly regulated and complex, and involves a variety of cell types

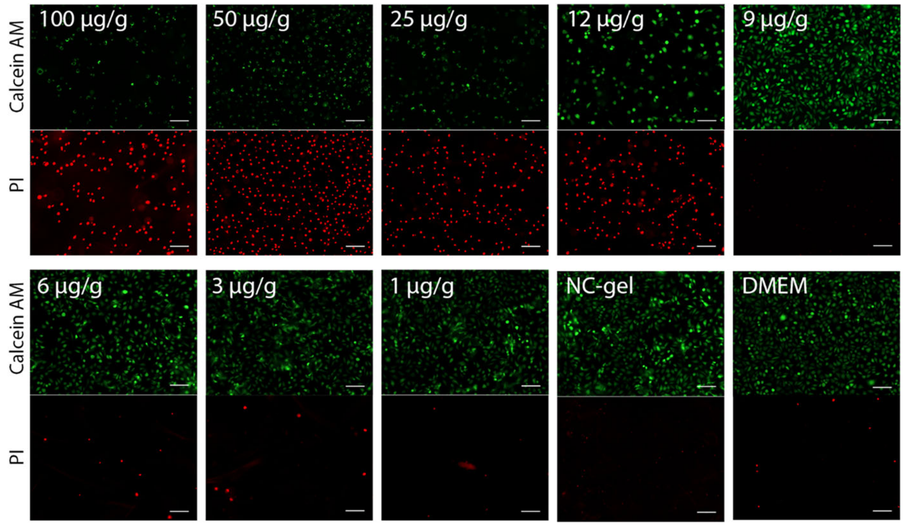

Fig. 5 Live-dead staining of L929 cells after 24 h of incubation with the indicated target concentration of the bismuth complex in nanocellulose hydrogel, the blank nanocellulose hydrogel (NC-gel) or DMEM culture media only. The green and red fluorescence show live and dead/dying cells respectively. Scale bar represents 100 µm

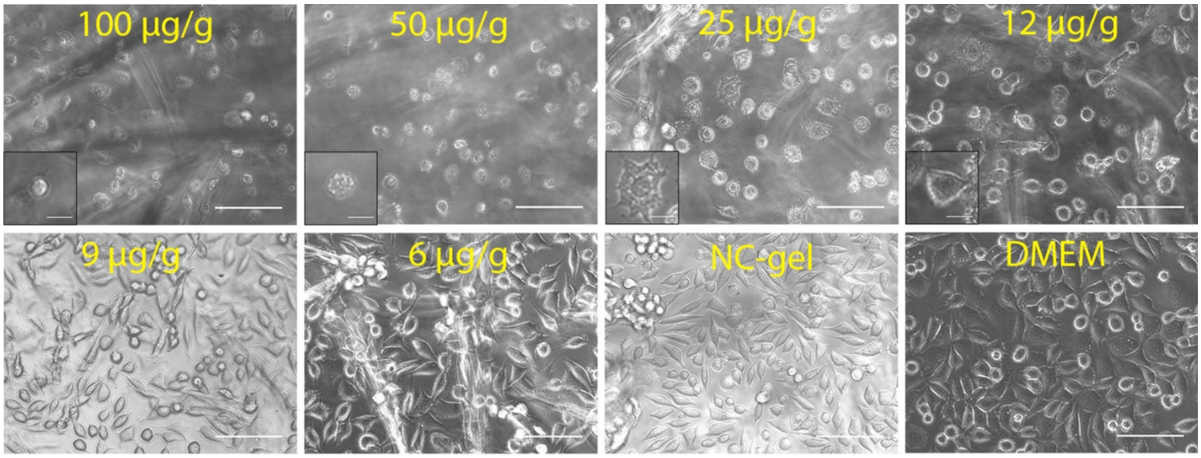

Fig. 6 Light microscopy of L929 cells after 24 h of incubation with the indicated target concentration of the bismuth complex in nanocellulose hydrogel, or blank nanocellulose hydrogel (NC-gel) without the bismuth complex or DMEM media only. Scale bar represents 100 µm in the images and 20 µm in the inset

including immune cells, fibroblasts and keratinocytes. Upon tissue injury, fibroblasts migrate into the wound and deposit extracellular matrix proteins such as collagen that is required for filling the injured site with newly synthesised tissue. As fibroblasts play a critical role in wound repair, it is important to evaluate the interactions of the cells with wound dressing materials, including potential cytotoxic effects (Tschumperlin 2013) (Wiegand et al. 2019). As per the ISO standard 10993-5, the cytotoxicity of the bismuth-loaded nanocellulose hydrogels was evaluated via assessing the cell viability of the murine fibroblast cell line L929. In addition, cytotoxicity was evaluated qualitatively via live-dead cell staining and morphological analysis. It is not clear how predictive the murine L929 cell line is of human fibroblast viability, but it is a widely employed cell line for cytotoxicity analysis and allows comparisons to other compounds. The vehicle, which is the pure nanocellulose hydrogel had no adverse effect on the fibroblast cells. The effect on cell viability of the bismuth-loaded gel was assessed using the MTS assay, live dead assay and the morphology of the mammalian cells. These experiments showed that at higher bismuth concentrations, the proportion of dead cells is increased, and hence viability is lower and the cell morphology deviates from normal. 12 μg/g was the highest concentration of bismuth complex which did not significantly reduce cell viability as determined by the MTS assay. However, in the live-dead assay and the morphology study, the cells showed no difference compared to controls at or below 9 μg/g loading of the bismuth complex. Further assays would be required to unequivocally demonstrate the safe bismuth loading for cells. However, results herein show that target concentrations of 9 μg/g bismuth complex appear to be well tolerated by the cells in-vitro. Similar in-vitro studies have shown that silver nanoparticles concentrations of 1.7 μg/ml, 5 μg/ml and 10 μg/ml have reduced viability on human epidermal keratinocytes (Samberg et al. 2010), rat liver cells (Hussain et al. 2005) and stem cells (Braydich-Stolle et al. 2005) respectively. Argyria occurs at levels greater than 2 μg/g (Khattak et al. 2009). In-vivo studies have also shown that silver nanoparticle exposure can affect different organs in mammals including liver and bile duct when ingested (Stensberg et al. 2011). Skin contact (porcine skin) causes swelling, increased size of epidermal layer of skin, inflammation and greyish color at concentration of 3.4 and 34 μg/ml (Samberg et al. 2010). It has been reported that many topical silver containing commercial products contain silver nanoparticles higher than 15 μg/g (Lee et al. 2015). Despite this, many silver-based hydrogel products are already approved in the commercial market. The limited safety data for the novel Bi-based hydrogel suggests it is worthy of further investigation as a potentially safe new material for wound management. However, further animal testing is imperative to better understand its clinical efficacy and effects on living organisms. The findings with approved commercial hydrogels tested herein tells us that these in-vitro performance differ significantly from a real-life scenario, thus suggesting that expanded biocompatibility assays will be required to adequately extrapolate to use in vivo.

Antibacterial activity

Time-kill assay

Time-kill assays were performed to understand the effect of concentration of the bismuth-complex loading at the safe concentrations established in the previous section against some common and significant wound pathogens. The time-kill kinetics in Fig. 7 shows that the Bi-loaded hydrogel is bactericidal within 4 h at 12 and 9 μg/g against the Gram-negative bacteria *A. baumannii*, rapidly eradicating bacterial colonies. However, the lower bismuth content (6 and 3 μg/g) remained bacteriostatic over the 24-h test period. When tested against *P. aeruginosa* (also Gram negative), bactericidal activity is observed within 8–12 h at 12 and 9 μg/g. At 6 μg/g, bactericidal activity is observed over the first 12 h, after which slow regrowth occurred. With the minimum loading of 3 μg/g, the bismuth complex was only able to slow down bacterial growth. Representative plates for *P. aeruginosa* are shown in Fig. S2. Interestingly, with the Gram-positive methicillin resistant strain of *Staphylococcus aureus* (MRSA) and Vancomycin-resistant *Enterococcus* (VRE), the trend observed was quite different. Bacteriostatic effects were observed upon treatment with 12, 9 or 6 μg/g of the complex up to 12 h for MRSA and 24 h for VRE. With MRSA, regrowth was observed at the above-mentioned concentrations after 12 h, with the regrowing rate and the final level of colony forming units being lower than the control after 24 h. With treatment of 3 μg/g, MRSA remained slow growing throughout the tested period. There was no reduction in bacterial colonies at any of the treatment concentrations (or times), thus indicating less activity of these hydrogels against these Gram-positive bacterial strains. Interestingly, the concentration dependency of *E. coli* was different to all the other bacteria tested, including the other Gram-negative ones. Important to note is that blank hydrogel (i.e. no bismuth additive) leads to a growth curve similar to medium alone and is shown in Fig. S3 in the supplementary information. Therein, the tests were done in hydrogel-broth mixture containing 20% w/w of the blank hydrogel or the Bi-loaded hydrogel.

Pseudomonas aeruginosa and *A. baumannii* have been identified as critical priority pathogens, followed by *E. coli,* VRE and MRSA as a high priority pathogens by the World Health Organization (World

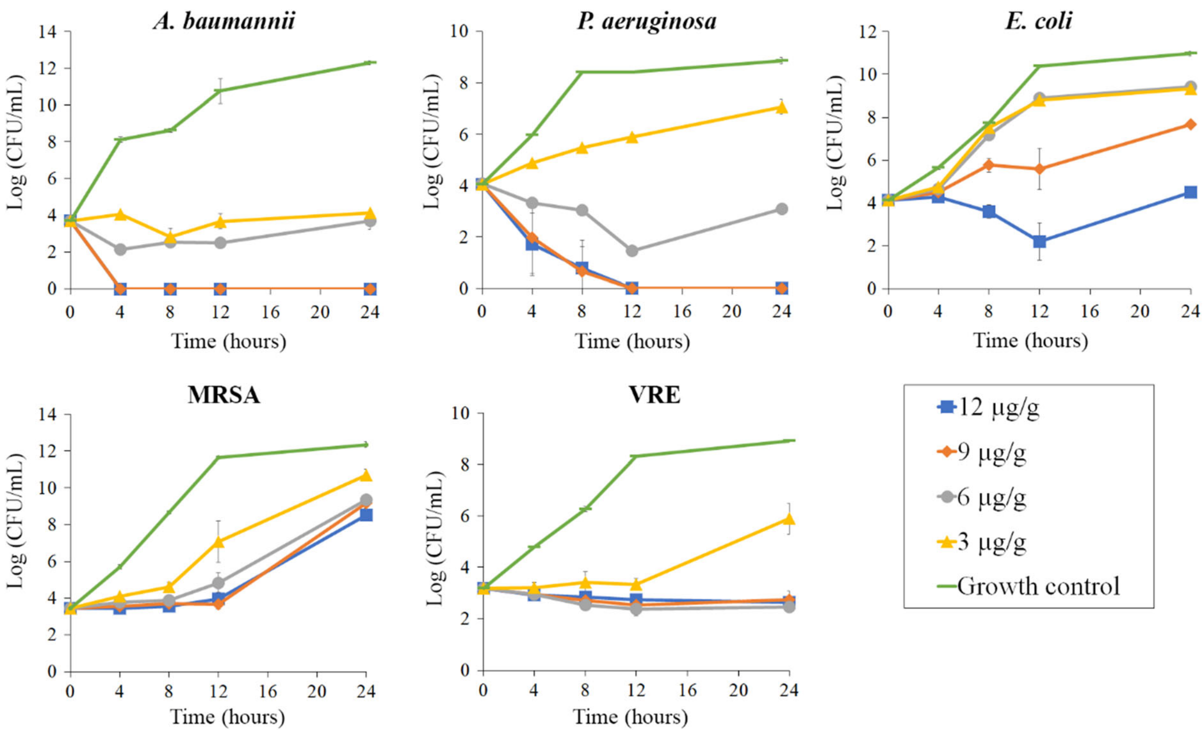

Fig. 7 Time-kill kinetics of the Bi-NC hydrogel at indicated target concentration of the bismuth complex against the Gram-negative bacterial strains of *A. baumannii*, *P. aeruginosa* and *E. coli* and the Gram-positive strains of MRSA and VRE for 24 h period. The values expressed represent mean ± standard deviation (n = 3). All measurements were done in triplicate and all data included except for the following three instances where two replicates were in agreement and one was an outlier, which was excluded: *A. baumannii* at 6 and 3 μg/g at 12 h *and P. aeruginosa* at 6 μg/g at 12 h

Health Organization 2017). These are responsible for the most common bacterial infections in burns (Norbury et al. 2016; Thabet et al. 2008). Around 12% of infections following burns are caused by *A. baumannii*, of which 99, 60 and 87% are resistant to ceftazidime, imipenem and ciprofloxacin respectively. *P. aeruginosa* infections, which comprise 16% of the total cases, have more than 35% of strains resistant to ceftazidime and imipenem. *S. aureus* still being the most common causative agent giving rise to 20% of all burn infections with 68% being methicillin resistant but susceptible to glycopeptides (Thabet et al. 2008). Infection from both *S. aureus* and *P. aeruginosa* are known to interfere with epithelization significantly, having a serious effect on the healing process (Pastar et al. 2014). Burn patients are at very high risk of MRSA infection, and combinations of infection control strategies are needed (Andrade et al. 2009). The bismuth complex loaded hydrogels studied herein showed rapid killing of the entire bacterial population of *P. aeruginosa* and *A. baumannii* at target concentrations of 12 and 9 μg/g within less than 24 h. However, with MRSA and VRE bacteriostatic effects were observed at these concentrations, followed by regrowth of MRSA after 12 h. Regrowth phenomena are common in time-kill studies (Sim et al. 2014). Mathematical models suggest these phenomena are indicative of adaptation and rapid evolution, which may be due to the presence of susceptible and resistant sub-populations within a bacterial strain (Tam et al. 2005).

Paradoxically, the bismuth containing hydrogels appear more active against Gram-negative bacteria. This is surprising because previous research with bismuth compounds has shown the opposite and found them more active against Gram positive bacteria (Kotani et al. 2005; Maliha et al. 2019; Werrett et al. 2018). The reasons for this are presently unknown however it may reflect improved availability of the complex for bacteria within a hydrogel matrix. This selectivity in the current formulation will limit its utility if a broad-spectrum agent is desired. However, this selectivity for target bacteria is commonly found among commercial hydrogels. A silver-based wound hydrogel containing 55 ppm of AgCl is not active against *P. aeruginosa* but is active against most Gram-positive bacteria (Lee et al. 2015). The silver-based commercial hydrogel, Silvasorb®, has a broader spectrum of action eliminating MRSA in 3 h, VRE in 2 h and *E. coli* in 6 h. Studies also suggests that it kills *P. aeruginosa* within 24 h, which is also true for our bismuth-NC hydrogel (Castellano et al. 2007). Broad spectrum antimicrobials have the benefit of being active against a range of bacteria, but have greater risks of selecting resistance genes. Narrow-spectrum antimicrobial agents may be preferred for treatment of skin infections, urinary tract infections and other non-life-threatening cases (Melander et al. 2018). It is encouraging that the current bismuth-hydrogel formulation targets two Gram-negative bacteria, a group that is generally more resistant and has fewer therapeutic options for treatment. However, *E. coli* showed to be an exception to this trend. In spite of being a Gram-negative bacterium, the bismuth complex was not successful in showing bactericidal activity at any concentrations tested. For Gram-negative bacteria, the permeability barrier by the cell wall is an important factor and depends on the efflux mechanism of a particular bacterial species and physicochemical properties of the antimicrobial agent (Zgurskaya et al. 2015). The bismuth-phosphinato antimicrobial agent studied herein is hydrophobic and present as large needle shaped particles in the hydrogel (Maliha et al. 2019). Hydrophobic compounds are generally transported into the cells of Gram-negative bacteria by passive diffusion. The structure of the outer membrane of *Pseudomonas* and *Acinetobacter* species are similar to most Gram-negative bacteria, except enterobacteria like *E. coli* (Zgurskaya et al. 2015). Species of *Acinetobacter* and *Pseudomonas* also showed higher permeability and more susceptibility than *E. coli* to large hydrophobic antibiotics like novobiocin, and erythromycin (Plésiat and Nikaido 1992). Moreover, *E. coli* has greater sensitivity to small molecule antibiotics compared to other Gram-negative ones. So the higher susceptibility of the more problematic bacterial species to the bismuth complex can be advantageous (Norbury et al. 2016). Reports indicate that *A. baumannii* uses hydrophobic compounds as growth nutrients and thus has a unique pathway for transport of hydrophobic substances into the cells (Borneleit and Kleber 1991). This transport pathway may explain the rapid bactericidal effect the Bi-complex had on *A. baumannii* within only 4 h. The concentration dependent activity of the hydrogel does suggest that higher concentrations of the bismuth complex may induce a bactericidal or sustained bacteriostatic effect for *E. coli*, MRSA and VRE. However, higher concentrations were not tested due to reduced mammalian cell viability.

Bacterial cell morphology

The hydrogel loaded with the bismuth complex is shown to have an effect on bacterial viability by time-kill kinetics. *P. aeruginosa* was taken as a model bacterium for this study, and bactericidal concentrations of 12 and 9 μg/g were studied. Untreated cells served as the control, which shows smooth surfaces on the rod-shaped bacterial cells, with no visible cell damage shown in Fig. 8a, b. Figure 8c shows the appearance of the cells after being treated with Bi-loaded hydrogels at 12 μg/g of the bismuth complex in the broth, with the cell surface having an uneven texture. Fibrous features formed on the exterior of the cells along with debris build-up around them. Figure 8b and d show the bacterial cells at the same magnification, clearly showing the difference in number of bacterial cells after being treated with Bi-loaded hydrogel with concentration of 9 μg/g of the bismuth complex compared to the control. Figure 9 shows the structure of a single bacterial cell to illustrate the morphological changes to individual cells after exposure to Bi-loaded hydrogels. The

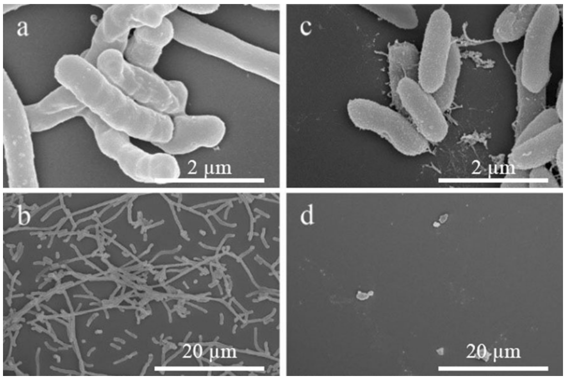

Fig. 8 SEM images of untreated *P. aeruginosa* cells (**a**, **b**), and treated with Bi-NC hydrogel with bismuth complex concentrations of 12 μg/g (**c**) and 9 μg/g (**d**)

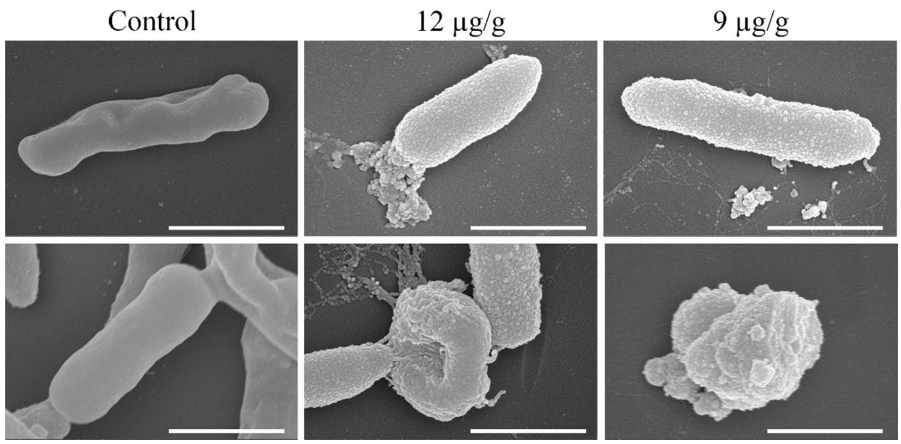

Fig. 9 SEM images of a single *P. aeruginosa* cell with no treatment (control), and treated with Bi-NC hydrogel with bismuth complex concentrations of 12 μg/g and 9 μg/g. Scale bar represents 1 μm

treated cells show obvious shape malformation, indicating possible disruption of the cell wall and/or loss of membrane integrity. When treated at 12 μg/g, intracellular material was observed to be leaking out of the cells, likely by formation of membrane bound vesicles. Overall, the cells show severe shape distortion and a crumpled surface after being treated, which supports the findings from the time-kill assay.

Internal quality control

Quality control tests were done to evaluate the reliability and reproducibility of the antibacterial test results. Blinded experimental repeats of the time-kill assays were performed using one Gram-positive (MRSA) and one Gram-negative (*A. baumannii*) bacteria in a different laboratory using a different batch of hydrogel. This was done to verify that the difference in activity towards these two classes of bacteria is reproducible, so one of each kind of bacteria was chosen. There were also some differences in the bacterial population in the blinded experiments in Fig. S4 compared to the original time-kill assay. This was true for both the 9 μg/g and the control growth curves. The control curve showed less growth in the blinded experiments. For instance, after 24 h MRSA showed 9 CFU/mL in the blinded experiment as opposed to 12 CFU/mL with the original time-kill assay. This could be because the interlaboratory repeatability of bacterial cell count using the CFU method is poor (Beal et al. 2020). However, the aim of this research was not to prove the interlaboratory reproducibility of the growth curve, but to show that the effect of the bismuth complex on the bacterial population compared to an untreated control at the same conditions is reproducible. The bacterial count showed similar fold reduction when treated with 9 μg/g Bi-complex compared to the control in the blinded repeats. For example, for MRSA, the ratio of the log CFU/mL of the control to the 9 μg/g at 4 h was 1.32 and 1.61 and at 24 h was 1.56 and 1.35 for the blinded experiment and the original experiment respectively. So, the bismuth complex was able to achieve a similar fold reduction. With the *A. baumannii*, the entire bacterial population was killed in 4 h, similar to the original assay. The interlaboratory reproducibility of the antibacterial activity proven from this study demonstrates the stability and reliability of the antibacterial activity of Bi-complex loaded hydrogels.

Hydrogel quality check

The 0.1 wt.% hydrogel was tested to verify the actual loading of the bismuth complex to account for all losses during the various stages of hydrogel preparation. It was found that the hydrogel contained 0.08 ± 0.01 wt.% of the bismuth complex, reported as batch 1 in Table S1. It is important to note that the actual bismuth content is somewhat lower than the target concentration. For applications like this, it is critical to ensure that the active agent concentration is consistent and predictable. A quality check study was performed to understand the bismuth complex content in different batches of hydrogels produced. The actual bismuth complex content of three more different batches of the bismuth-loaded hydrogel were tested, as shown in Table S1. The average ± standard deviation of the bismuth complex content in the four batches of hydrogels was 0.081 ± 0.002 wt.%, showing that a consistent loading was achieved.

The studies reported here identify a bismuth complex loading of 9 µg/g as the most appropriate concentration for further study. Concentrations of 12 and 9 µg/g do not show much difference in antibacterial activity to the most bacterial strains tested. The cytotoxicity assays suggest there is a measurable deleterious effect on fibroblasts at 12 µg/g and above compared to the DMEM control. Lower concentrations do not decrease cellular proliferation or viability of the fibroblast line tested. From this comparison, a target concentration of 9 µg/g is identified as the optimum concentration, showing toxicity to prokaryotic bacterial cells (of Gram-negative type in particular) along with having no adverse effect on mammalian cells. According to the ICP-OES analysis the actual bismuth complex content is slightly, yet consistently, lower than the target loading. The optimised target concentration of 9 µg/g (9.375 µg/g in 3 decimal places) is calculated to contain 7.5 µg/g. The actual bismuth content quality check must be performed prior to commercial production. The bismuth complex is highly hydrophobic and tends to stick to beaker walls and other surfaces during the Bi-loaded hydrogel preparation resulting in lower than the target loading. This makes it difficult to synthesize a hydrogel with such low concentration at laboratory scale. Once incorporated into a nanocellulose matrix, the complex particles are intertwined by the fibres which protect them from coming out onto the surfaces. Moreover, the limitation of in-vitro tests is that the sample must be diluted in media and it is this treatment mixture of sample and media that is delivered to the cells. Therefore, the bismuth content in the treatment mixture and the prepared (neat) hydrogel will be different. Hence, a single batch of hydrogel was prepared for which the actual bismuth content was measured. The Bi-hydrogel was diluted to study the effect of different concentrations of the complex. Future work should include testing a 9 µg/g loaded nanocellulose hydrogel on an in-vivo skin model. Since the pure nanocellulose hydrogel was shown to be non-toxic, the toxic effect in the bismuth-loaded hydrogels was solely due to the bismuth complex content which has been optimised in this paper. Thus, nanocellulose hydrogel loaded with a target concentration of 9 µg/g bismuth complex is the most appropriate concentration for further study as antibacterial wound dressing that can lessen the bioburden, thereby reducing the probability of wounds becoming infected. In addition, the highly hydrated nature of the hydrogel can promote wound healing.

Conclusion

The potential of phenyl *bis*-diphenylphosphinato bismuth (III) complex loaded nanocellulose hydrogels for wound care applications has been investigated. Morphological studies using SEM show a well-distributed complex in the hydrogel matrix. The rheological properties show the hydrogel behaves like true gels and is comparable to commercial burn hydrogels sold in tubes. This highlights the suitability of our material in terms of ease of storage and application. An extensive study to optimise the loading of the bismuth complex in the hydrogel was done. It was shown there is a dose-dependent effect on both the antibacterial properties as well as the toxicity toward mammalian fibroblast cells. The study herein gives a detailed understanding of the host-cell safety and antibacterial activity of different levels of the bismuth complex in the hydrogel matrix. The optimum target concentration of 9 µg/g was established to have a selective toxicity towards bacteria over mammalian cells. This study demonstrates that these hydrogels can be promising candidates as antimicrobial wound gels when the bismuth complex is used at safe but active levels. This opens opportunities for formulation of a renewable, safe and active wound care hydrogel using a new class of antibacterial agent to address the issue of rising antimicrobial resistance. Moreover, the bactericidal behaviour of the complex towards the Gram-negative bacterial strains, *A. baumannii* and *P. aeruginosa*, at concentrations safe to host cells is promising, given therapeutics for treatment of infections caused by these bacteria are limited (Norbury et al. 2016). The antibacterial selectivity towards the different bacterial strains suggests its usefulness in specific clinical utility over a broad-spectrum antibacterial material. This might be advantageous over silver wound gels, which are generally broad-spectrum antibacterial materials (Lee et al. 2015). However, our study here is limited to in-vitro experiments of the biocompatibility and antibacterial effect. The in-vitro results presented in this paper provides a useful preliminary screening to optimise Bi-nanocellulose hydrogel formulation and future in-vivo studies on animal models is required using hydrogel loaded with the optimised level of bismuth complex for regulatory purposes. An infected wound model is highly recommended to understand not only the biocompatibility and antibacterial activity of the composite hydrogel, but also to understand the healing properties of the hydrogel.

Acknowledgments The authors thank Monash University and The National Health and Medical Research Council (APP1139844) for financial support. The authors would like to acknowledge the use of the facilities in the Monash Centre for Electron Microscopy and Ramaciotti Centre for Cryo-Electron Microscopy. The authors would like to thank Dr. Simon Crawford for his assistance. Maisha Maliha would like to acknowledge the Australian Government for the Research Training Program (RTP) Scholarship.

Author contributions Conceptualization: MM, MW, PA, WB; Methodology: MM, JD; Investigation: MM, RB; Formal analysis: MM; Writing—original draft preparation: MM; Writing—review and editing: MM, RB, JD, RLC, MW, PCA, WB; Funding acquisition: WB; Resources: JD, RC, PCA, WB; Supervision: MW, PCA, WB.

Funding The National Health and Medical Research Council (APP1139844).

Data availability https://doi.org/10.26180/5f7b1a1262a02.

Declarations

Conflict of interest The authors declare that they have no conflicts of interest to declare.

References

Abou-Yousef H, Kamel S (2015) High efficiency antimicrobial cellulose-based nanocomposite hydrogels. J Appl Polym Sci. https://doi.org/10.1002/app.42327

Agyingi E, Maggelakis S, Ross D (2010) The effect of bacteria on epidermal wound healing. Math Model Nat Phenom 5:28–39. https://doi.org/10.1051/mmnp/20105303

Andrade C, Champagne S, Caruso D, Foster K, Reynolds K (2009) Methicillin-resistant Staphylococcus aureus: an assessment of environmental contamination in a burn center. Am J Infect Control 37:515–517. https://doi.org/10.1016/j.ajic.2008.10.026

Ashtikar M, Wacker M (2018) Nanopharmaceuticals for wound healing: Lost in translation? Adv Drug Deliv Rev. https://doi.org/10.1016/j.addr.2018.03.005

Babu VR, Kim C, Kim S, Ahn C, Lee YI (2010) Development of semi-interpenetrating carbohydrate polymeric hydrogels embedded silver nanoparticles and its facile studies on *E. coli*. Carbohydr Polym 81:196–202. https://doi.org/10.1016/j.carbpol.2010.02.050

Bardajee GR, Hooshyar Z, Rezanezhad H (2012) A novel and green biomaterial based silver nanocomposite hydrogel: synthesis, characterization and antibacterial effect. J Inorganic Biochem 117:367–373. https://doi.org/10.1016/j.jinorgbio.2012.06.012

Barry NPE, Sadler PJ (2013) Exploration of the medical periodic table: towards new targets. Chem Commun 49:5106–5131. https://doi.org/10.1039/c3cc41143e

Barton DHR, Bhatnagar NY, Finet J-P, Motherwell WB (1986) Pentavalent organobismuth reagents. Part VI Comparative migratory aptitudes of aryl groups in the arylation of phenols and enols by pentavalent bismuth reagents. Tetrahedron 42:3111–3122. https://doi.org/10.1016/S0040-4020(01)87378-6

Basu A, Lindh J, Ålander E, Strømme M, Ferraz N (2017) On the use of ion-crosslinked nanocellulose hydrogels for wound healing solutions: Physicochemical properties and application-oriented biocompatibility studies. Carbohydr Polym 174:299–308. https://doi.org/10.1016/j.carbpol.2017.06.073

Basu A, Heitz K, Strømme M, Welch K, Ferraz N (2018) Ion-crosslinked wood-derived nanocellulose hydrogels with tunable antibacterial properties: Candidate materials for advanced wound care applications. Carbohydr Polym 181:345–350. https://doi.org/10.1016/j.carbpol.2017.10.085

Beal J et al (2020) Robust estimation of bacterial cell count from optical density. Commun Biol 3:512. https://doi.org/10.1038/s42003-020-01127-5

Borneleit P, Kleber HP (1991) The Outer Membrane of Acinetobacter: Structure-Function Relationships. In: Towner KJ, Bergogne-Bérézin E, Fewson CA (eds) The Biology of Acinetobacter: Taxonomy, Clinical Importance, Molecular Biology, Physiology, Industrial Relevance. Springer, Boston. https://doi.org/10.1007/978-1-4899-3553-3_18

Braydich-Stolle L, Hussain S, Schlager JJ, Hofmann M-C (2005) vitro cytotoxicity of nanoparticles in mammalian germline stem cells. Toxicol Sci 88:412–419. https://doi.org/10.1093/toxsci/kfi256

Briand GG, Burford N (1999) Bismuth compounds and preparations with biological or medicinal relevance. Chem Rev 99:2601–2658. https://doi.org/10.1021/cr980425s

Caló E, Khutoryanskiy VV (2015) Biomedical applications of hydrogels: a review of patents and commercial products. Eur Polymer J 65:252–267. https://doi.org/10.1016/j.eurpolymj.2014.11.024

Castellano JJ et al (2007) Comparative evaluation of silver-containing antimicrobial dressings and drugs. Int Wound J 4:139–140. https://doi.org/10.1111/j.1742-481X.2007.00316.x

Chinga-Carrasco G, Syverud K (2014) Pretreatment-dependent surface chemistry of wood nanocellulose for pH-sensitive hydrogels. J Biomater Appl 29:423–432. https://doi.org/10.1177/0885328214531511

Cushen M, Kerry J, Morris M, Cruz-Romero M, Cummins E (2012) Nanotechnologies in the food industry: Recent developments, risks and regulation. Trends Food Sci Technol 24:30–46. https://doi.org/10.1016/j.tifs.2011.10.006

Czaja W, Krystynowicz A, Bielecki S, Brown RM (2006) Microbial cellulose—the natural power to heal wounds. Biomaterials 27:145–151. https://doi.org/10.1016/j.biomaterials.2005.07.035

De France K, Hoare T, Cranston E (2017) Review of hydrogels and aerogels containing nanocellulose. Chemistry Material. https://doi.org/10.1021/acs.chemmater.7b00531

Domenico P, Baldassarri L, Schoch PE, Kaehler K, Sasatsu M, Cunha BA (2001) Activities of Bismuth Thiols against staphylococci and staphylococcal biofilms. Antimicrob Agents Chemother 45:1417

Finland : UPM's FibDex, a wood-based innovation for wound care, receives regulatory approval and CE mark (2019). Mena Report

Fukuzumi H, Saito T, Iwata T, Kumamoto Y, Isogai A (2009) Transparent and High Gas Barrier Films of Cellulose Nanofibers Prepared by TEMPO-Mediated Oxidation. Biomacromol 10:162–165. https://doi.org/10.1021/bm801065u

Ghallab A (2013) In vitro test systems and their limitations. EXCLI J 12:1024–1026

González-Sánchez MI, Perni S, Tommasi G, Morris NG, Hawkins K, López-Cabarcos E, Prokopovich P (2015) Silver nanoparticle based antibacterial methacrylate hydrogels potential for bone graft applications. Mater Sci Eng C 50:332–340. https://doi.org/10.1016/j.msec.2015.02.002

Gunawan C, Marquis CP, Amal R, Sotiriou GA, Rice SA, Harry EJ (2017) Widespread and Indiscriminate Nanosilver Use: Genuine Potential for Microbial Resistance. ACS Nano 11:3438. https://doi.org/10.1021/acsnano.7b01166

Güzel Bayülken D, Ayaz Tüylü B (2019) vitro genotoxic and cytotoxic effects of some paraben esters on human peripheral lymphocytes. Drug Chem Toxicol 42:386–393. https://doi.org/10.1080/01480545.2018.1457049

Hakkarainen T et al (2016) Nanofibrillar cellulose wound dressing in skin graft donor site treatment. J Control Release 244:292–301. https://doi.org/10.1016/j.jconrel.2016.07.053

Hartung T, Daston G (2009) Are in vitro tests suitable for regulatory use? Toxicol Sci 111:233–237. https://doi.org/10.1093/toxsci/kfp149

Hebeish A, Hashem M, El-Hady MMA, Sharaf S (2013) Development of CMC hydrogels loaded with silver nanoparticles for medical applications. Carbohydr Polym 92:407–413. https://doi.org/10.1016/j.carbpol.2012.08.094

Hussain SM, Hess KL, Gearhart JM, Geiss KT, Schlager JJ (2005) In vitro toxicity of nanoparticles in BRL 3A rat liver cells. Toxicol in Vitro 19:975–983. https://doi.org/10.1016/j.tiv.2005.06.034

Jones V, Grey J, Harding K (2006) Wound dressings. Br Med J 332:777

Kamoun EA, Kenawy E-RS, Chen X (2017) A review on polymeric hydrogel membranes for wound dressing applications: PVA-based hydrogel dressings. J Adv Res 8:217–233. https://doi.org/10.1016/j.jare.2017.01.005

Khattak AZ, Ross R, Ngo T, Shoemaker CT (2009) A randomized controlled evaluation of absorption of silver with the use of silver alginate (Algidex) patches in very low birth weight (VLBW) infants with central lines. J Perinatol 30:337. https://doi.org/10.1038/jp.2009.169

Kotani T, Nagai D, Asahi K, Suzuki H, Yamao F, Kataoka N, Yagura T (2005) Antibacterial properties of some cyclic Organobismuth(III) compounds. Antimicrob Agents Chemother 49:2729. https://doi.org/10.1128/AAC.7.2729-2734.2005

Laçin NT (2014) Development of biodegradable antibacterial cellulose based hydrogel membranes for wound healing. Int J Biol Macromol 67:22–27. https://doi.org/10.1016/j.ijbiomac.2014.03.003

Lee Y, Atchley DH, Proctor CA, Smith FL, Yi S, Loftis CM, Yates KM (2015) Time-kill Kinetics of a Novel Antimicrobial Silver Wound Gel Against Select Wound Pathogens Wounds: a compendium of clinical research and practice. Eur J Inorg Chem 27:336–346

Luqman A, Blair VL, Brammananth R, Crellin PK, Coppel RL, Andrews PC (2016) The importance of heterolepticity in improving the antibacterial activity of Bismuth(III) thiolates. Eur J Inorg Chem 2016:2738–2749. https://doi.org/10.1002/ejic.201600076

Maillard J-Y, Hartemann P (2013) Silver as an antimicrobial: facts and gaps in knowledge. Crit Rev Microbiol 39:373–383. https://doi.org/10.3109/1040841X.2012.713323

Maliha M et al (2019) Bismuth phosphinate incorporated nanocellulose sheets with antimicrobial and barrier properties for packaging applications. J Cleaner Prod. https://doi.org/10.1016/j.jclepro.2019.119016

Maneerung T, Tokura S, Rujiravanit R (2008) Impregnation of silver nanoparticles into bacterial cellulose for antimicrobial wound dressing. Carbohydr Polym 72:43–51. https://doi.org/10.1016/j.carbpol.2007.07.025

Melander RJ, Zurawski DV, Melander C (2018) Narrow-spectrum antibacterial agents. Medchemcomm 9:12–21. https://doi.org/10.1039/C7MD00528H

Mendoza L, Batchelor W, Tabor RF, Garnier G (2018) Gelation mechanism of cellulose nanofibre gels: a colloids and interfacial perspective. J Colloid Interface Sci 509:39–46. https://doi.org/10.1016/j.jcis.2017.08.101

Norbury W, Herndon DN, Tanksley J, Jeschke MG, Finnerty CC (2016) Infection in Burns. Surg Infect 17:250–255. https://doi.org/10.1089/sur.2013.134

Pastar I et al (2014) Epithelialization in Wound Healing: A Comprehensive Review. Adv Wound Care 3:445–464. https://doi.org/10.1089/wound.2013.0473

Plésiat P, Nikaido H (1992) Outer membranes of gram-negative bacteria are permeable to steroid probes. Mol Microbiol 6:1323–1333. https://doi.org/10.1111/j.1365-2958.1992.tb00853.x

Rattanaruengsrikul V, Pimpha N, Supaphol P (2009) Development of gelatin hydrogel pads as antibacterial wound dressings. Macromol Biosci 9:1004–1015. https://doi.org/10.1002/mabi.200900131

Resmi R, Unnikrishnan S, Krishnan LK, Kalliyana Krishnan V (2017) Synthesis and characterization of silver nanoparticle incorporated gelatin-hydroxypropyl methacrylate hydrogels for wound dressing applications. J Appl Polym Sci. https://doi.org/10.1002/app.44529

Restuccia D, Salomone R, Spizzirri UG, Saija G, Ioppolo G, Parisi OI, Picci N (2016) Industrial Applications: Regulatory issues and life cycle assessment of food packaging, chap 16. Elsevier Inc. https://doi.org/10.1016/B978-0-12-800723-5.00016-4

Saito T, Kimura S, Nishiyama Y, Isogai A (2007) Cellulose nanofibers prepared by TEMPO-mediated oxidation of native cellulose. Biomacromol 8:2485. https://doi.org/10.1021/bm0703970

Samberg ME, Oldenburg SJ, Monteiro-Riviere NA (2010) Evaluation of silver nanoparticle toxicity in skin in vivo and keratinocytes in vitro. Environ Health Perspect 118:407–413. https://doi.org/10.1289/ehp.0901398

Shpichka A et al (2019) Skin tissue regeneration for burn injury. Stem Cell Res Therapy 10:94. https://doi.org/10.1186/s13287-019-1203-3

Silver S (2003) Bacterial silver resistance: molecular biology and uses and misuses of silver compounds. FEMS Microbiol Rev 27:341–353. https://doi.org/10.1016/S0168-6445(03)00047-0

Sim J-H, Jamaludin NS, Khoo C-H, Cheah Y-K, Halim SNBA, Seng H-L, Tiekink ERT (2014) In vitro antibacterial and time-kill evaluation of phosphanegold(I) dithiocarbamates, $R_3PAu[S_2CN(iPr)CH_2CH_2OH]$ for R = Ph Cy and Et, against a broad range of Gram-positive and Gram-negative bacteria. Gold Bull 47:225–236. https://doi.org/10.1007/s13404-014-0144-y

Singh R, Singh D (2012) Radiation synthesis of PVP/alginate hydrogel containing nanosilver as wound dressing. Off J Eur Soc Biomater 23:2649–2658. https://doi.org/10.1007/s10856-012-4730-3

Spindola DG, Hinsberger A, Antunes VMdS, Michelin LFG, Bincoletto C, Oliveira CR (2018) In vitro cytotoxicity of chemical preservatives on human fibroblast cells. Braz J Pharm Sci. https://doi.org/10.1590/s2175-97902018000100031

Stensberg MC, Wei Q, McLamore ES, Porterfield DM, Wei A, Sepulveda MS (2011) Toxicological studies on silver nanoparticles: challenges and opportunities in assessment, monitoring and imaging. Nanomedicine (Lond) 6:879–898. https://doi.org/10.2217/nnm.11.78

Suzuki H, Matano Y (2001) Chapter 1: Introduction. In: Matano Y (ed) Organobismuth Chemistry. Elsevier, Amsterdam. https://doi.org/10.1016/B978-044420528-5/50003-3

Svoboda T, Jambor R, Ruzicka A, Padelkova Z, Erben M, Dostal L (2010) NCN Chelated Organoantimony(III) and Organobismuth(III) Phosphinates and Phosphites: Synthesis Structure and Reactivity. Eur J Inorg Chem 2010:5222–5230. https://doi.org/10.1002/ejic.201000746

Tam VH, Schilling AN, Nikolaou M (2005) Modelling time–kill studies to discern the pharmacodynamics of meropenem. J Antimicrob Chemother 55:699–706. https://doi.org/10.1093/jac/dki086

Thabet L, Turki A, Ben Redjeb S, Messadi A (2008) Bacteriological profile and antibiotic resistance of bacteria isolates in a burn department. Tunis Med 86:1051–1054

Thomas V, Yallapu MM, Sreedhar B, Bajpai SK (2007) A versatile strategy to fabricate hydrogel–silver nanocomposites and investigation of their antimicrobial activity. J Colloid Interface Sci 315:389–395. https://doi.org/10.1016/j.jcis.2007.06.068

Tschumperlin DJ (2013) Fibroblasts and the ground they walk on. Physiology 28:380–390. https://doi.org/10.1152/physiol.00024.2013

Tyliszczak B, Drabczyk A, Kudłacik-Kramarczyk S, Bialik-Wąs K, Kijkowska R, Sobczak-Kupiec A (2017) Preparation and cytotoxicity of chitosan-based hydrogels modified with silver nanoparticles. Colloids Surf B 160:325–330. https://doi.org/10.1016/j.colsurfb.2017.09.044

Valle H, Rivas B, Fernandez M, Mondaca M, Aguilar M, Roman J (2014) Antibacterial activity and cytotoxicity of hydrogel-nanosilver composites based on copolymers from 2-acrylamido-2-methylpropanesulfonate sodium Journal of Applied Polymer Science 131 doi:https://doi.org/10.1002/app.39644

Werrett M et al (2018) Bismuth phosphinates in Bi-nanocellulose composites and their efficacy towards multi-drug resistant bacteria chemistry- a. Eur J. https://doi.org/10.1002/chem.201801803

World Health Organization (2017) Prioritization of pathogens to guide discovery, research and development of new antibiotics for drug resistant bacterial infections, including tuberculosis. World Health Organization, Geneva (WHO/EMP/IAU/2017.12). (Licence: CC BY-NC-SA 3.0 IGO)

Wiegand C, Abel M, Hipler U-C, Elsner P (2019) Effect of non-adhering dressings on promotion of fibroblast proliferation and wound healing in vitro. Sci Rep 9:4320. https://doi.org/10.1038/s41598-019-40921-y

Zgurskaya HI, Löpez CA, Gnanakaran S (2015) Permeability barrier of gram-negative cell envelopes and approaches to bypass it ACS. Infect Dis 1:512–522. https://doi.org/10.1021/acsinfecdis.5b00097